

## Supplementary Information

# Enhancing the Electroreduction of N<sub>2</sub> and/or O<sub>2</sub> on MoS<sub>2</sub> using a Nanoparticulate Intrinsically Microporous Polymer (PIM-1)

Caio V. S. Almeida,<sup>1,2</sup> Lara K. Riberio,<sup>1,2</sup> Lucia H. Mascaro,\*<sup>1</sup> Mariolino Carta,<sup>3</sup> Neil B. McKeown,<sup>4</sup> Frank Marken\*<sup>2</sup>

<sup>1</sup> *Department of Chemistry, Federal University of São Carlos, Zip Code 13565-905, São Carlos, SP, Brazil*

<sup>2</sup> *Department of Chemistry, University of Bath, Claverton Down, Bath BA2 7AY, UK*

<sup>3</sup> *Department of Chemistry, Swansea University, College of Science, Grove Building, Singleton Park, Swansea SA2 8PP, UK*

<sup>4</sup> *EaStCHEM, School of Chemistry, University of Edinburgh, Joseph Black Building, David Brewster Road, Edinburgh, Scotland EH9 3JF, UK*

## Content

<b>Experimental</b> .....	<b>3</b>
<b>Reagents</b> .....	<b>3</b>
<b>Instrumentation</b> .....	<b>3</b>
<b>Procedures</b> .....	<b>4</b>
<b>Figure S1.</b> Calibration curve for estimating H <sub>2</sub> O <sub>2</sub> concentration, (b) corresponding Counts versus Acquisition time for LC-MS of resultant solutions. ....	<b>8</b>
<b>Figure S2.</b> (a) Photograph of different concentrations of NH <sub>3</sub> stained with the indophenol indicator, (b) corresponding counts versus acquisition time for LC-MS of resultant solutions and (c) calibration of the indophenol blue method for estimating NH <sub>3</sub> concentration, using NH <sub>4</sub> Cl solutions of known concentration as standards calibration. ....	<b>9</b>
<b>Figure S3.</b> (a) Cyclic voltammograms (scan rate 50 mV s <sup>-1</sup> ) for carbon paper, MoS <sub>2</sub> /CP and PIM-1 <sub>(120 μg)</sub> /MoS <sub>2</sub> (inset) in O <sub>2</sub> -saturated 0.1 mol L <sup>-1</sup> phosphate buffer pH 7. (b) Cyclic voltammograms (scan rate 50 mV s <sup>-1</sup> ) for carbon paper in 0.1 mol L <sup>-1</sup> phosphate buffer pH 7 at different gas environments. ....	<b>10</b>
<b>Figure S4.</b> Calibration of the Watt and Chrisp method for estimating N <sub>2</sub> H <sub>4</sub> concentration, using N <sub>2</sub> H <sub>4</sub> solutions of known concentration as standards. (a) UV-Vis curves of various N <sub>2</sub> H <sub>4</sub> concentration after incubated for 30 min at room temperature. The absorbance at 455 nm was measured by UV-Vis spectrophotometer (b) calibration curve used for estimation of N <sub>2</sub> H <sub>4</sub> concentration. (c) UV-vis absorption spectra of the electrolyte stained with Watt and Chrisp indicator after NRR electrolysis using PIM-1 <sub>(120 μg)</sub> /MoS <sub>2</sub> /CP at -0.85 V vs. Ag/AgCl. ....	<b>11</b>
<b>Table S1.</b> Comparison of optimum NH <sub>3</sub> yield rates and Faradaic efficiency (FE) for several catalysts for NRR at ambient conditions. ....	<b>12</b>
<b>Figure S5.</b> (a) NH <sub>3</sub> yield rate and FE values and (b) corresponding counts versus acquisition time for LC-MS for electrolytes with indophenol indicator obtained at different potentials for MoS <sub>2</sub> /CP catalyst. ....	<b>13</b>
<b>Figure S6.</b> (a) Corresponding counts versus acquisition time for LC-MS data for indophenol indicator from ammonia and (b) NH <sub>3</sub> Yield rate comparison using <sup>14</sup> N <sub>2</sub> and <sup>15</sup> N <sub>2</sub> as the feeding gas for PIM-1 <sub>(120 μg)</sub> /MoS <sub>2</sub> /CP at -0.85 V vs. Ag/AgCl. ....	<b>14</b>
<b>Figure S7.</b> Comparison of NH <sub>3</sub> yield rate and LC chromatogram for indophenol and MS mass signal for 2 h electrolysis (i) PBS 0.1 mol L <sup>-1</sup> under ambient air, (ii) using bare carbon paper electrodes in ambient air, (iii) without current flow under ambient air, and (iv) applying -0.85 V vs. Ag/AgCl in PIM-1 <sub>(120 μg)</sub> /MoS <sub>2</sub> /CP. In cases (i to iii), the ammonia detection remains negligible in comparison with reaction in PIM-1 <sub>(120 μg)</sub> /MoS <sub>2</sub> /CP. ....	<b>15</b>

<b>Figure S8.</b> Counts versus acquisition time measurements after six chronoamperometric runs for PIM-1 <sub>(120 μg)</sub> /MoS <sub>2</sub> /CP at -0.85 V vs. Ag/AgCl. ....	<b>16</b>
<b>Figure S9.</b> SEM images (a) before and (b) after stability test and (c) Raman spectra (532 nm) before and after stability test for PIM-1 <sub>(120 μg)</sub> /MoS <sub>2</sub> /CP. ....	<b>17</b>
<b>References</b> .....	<b>18</b>

## Experimental

**Reagents.** Ammonium tetrathiomolybdate (99.97%), sodium perchlorate (≥98%), monobasic sodium phosphate (≥98%), dibasic sodium phosphate (≥99.0%), para-(dimethylamino) benzaldehyde (p-C<sub>9</sub>H<sub>11</sub>NO), phenol (≥99%), sodium nitroprusside (≥99.0%), sodium hydroxide (≥97.0%), sodium hypochlorite aqueous solution (6-14 % active chlorine), concentrated hydrochloric acid (HCl - 37 wt %) sulfuric acid (H<sub>2</sub>SO<sub>4</sub> – 98%), nitric acid (HNO<sub>3</sub> – 65%), methanol, ethanol and chloroform were obtained from Sigma-Aldrich and used without further purification. PIM-1 (or 2,3,5,6-tetrafluorophthalonitrile-3,3,3',3'- tetramethyl-1,1'- spirobisindane- 5,5',6,6'-tetrol copolymer, Sigma Aldrich, monomer molecular weight 460 g mol<sup>-1</sup>, molecular weight typically 70 KD) was synthesized using a method described in the literature.<sup>[42,43]</sup> A carbon paper (TGP-H-090 - total thickness of 280 μm) was obtained from Toray Industries. Argon, nitrogen and oxygen were purchased from BOC UK (Pureshield). Ultrapure water (18.2 MΩ cm at 20 °C) obtained from a Thermo Scientific water purification system, was used to prepare all solutions.

**Instrumentation.** A potentiostat/galvanostat (Autolab Model GPSTAT12, EcoChemie, The Netherlands) with a three-electrode system was used to carry out all the electrochemical measurements. The working electrodes on carbon paper (CP) were MoS<sub>2</sub>/CP and PIM-1/MoS<sub>2</sub>/CP, while a graphite rod was used as counter electrode in a separate compartment (separated by a glass frit), and a KCl (4 M) Ag/AgCl was employed as reference (Fisher Scientific,  $E$  (vs RHE) =  $E_{\text{appl}}$  (vs. Ag/AgCl/Cl<sub>(4M KCl)</sub>) + pH × 0.059 V + 0.197 V). The error in potential due to junction potentials and temperature is approx. ± 10 mV. A 0.1 mol L<sup>-1</sup> phosphate buffer solution (PBS; sodium-based) pH 7 was used

as the electrolyte solution for all experiments. The MoS<sub>2</sub>/CP and PIM-1/MoS<sub>2</sub>/CP catalysts were characterized using a field emission scanning electron microscope (FE-SEM, Jeol JSM-7900F) with an acceleration voltage of 5.0 kV. XRD patterns were collected in a STOE STADI P equipped with a Multi-Mythen detector using monochromated Cu K $\alpha$  radiation (1.54060 Å). The ammonia production was analyzed on a reverse phase ion-pairing chromatography coupled to tandem mass spectrometry (Agilent 6545 Accurate-Mass Q-TOF LC/MS system). A Walkup mass spectrometer was used for mass detection with a fragmentor voltage of 80 V and collision energy of 30 V. Peaks were integrated in Mass Hunter (Agilent) software.

## Procedures

*Pre-treatment of carbon paper.* Before the deposition of the catalysts, the carbon paper substrate needed to be treated in acid to increase the hydrophilicity of the material, which is hydrophobic due to the presence of PTFE on the surface. For the acid treatment method, concentrated H<sub>2</sub>SO<sub>4</sub>/HNO<sub>3</sub> (V/V:3/1) solution were prepared. The CP (0.5 cm  $\times$  0.5 cm on both sides to give approximately 0.5 cm<sup>2</sup> total geometric electrode area) was dropped into the acid solution and subjected to an ultrasonic cleaning bath for 10 min at room temperature. Then, the substrate was rinsed multiple times with ultrapure water and dried in the oven at 60 °C for 1 hour.

*Synthesis of MoS<sub>2</sub> (MoS<sub>2</sub>/CP).* The molybdenum sulfide film was prepared by electrodeposition technique according to previous reports.<sup>[56-58]</sup> The cyclic voltammetry (CV) technique was performed for 50 cycles in the potential range of -1.1 V to 0.2 V vs. Ag/AgCl at 50 mV s<sup>-1</sup> using 5 mmol L<sup>-1</sup> (NH<sub>4</sub>)<sub>2</sub>MoS<sub>4</sub> and 0.1 mol L<sup>-1</sup> NaClO<sub>4</sub>, previously de-aerated with Ar for 15 min.

*PIM-1 nanoparticle synthesis.* PIM-1 nanoparticles were synthesized using an anti-solvent precipitation method, as reported previously.<sup>[59,60]</sup> Briefly, the PIM-1 polymer was dissolved in 2 mL of chloroform at a concentration of 1 mg mL<sup>-1</sup>. The solution was added dropwise into 20 mL of methanol with vigorous stirring for 30 min, followed by centrifugation for 30 min at 5000 rpm for the removal of excess methanol. The PIM-1 nanoparticles were subsequently re-dispersed in methanol by ultrasonication (15 min). To

prepare nanoparticle films, a volume of 5  $\mu\text{L}$  (2 mg  $\text{mL}^{-1}$ ) of PIM-1 solution in methanol, equivalent to 10  $\mu\text{g}$  PIM-1 (other quantities of PIM-1 used in this study were calculated proportionally), was drop-coated onto the  $\text{MoS}_2/\text{CP}$  electrode to dry at room temperature.

*O<sub>2</sub> reduction reaction (ORR).* Cyclic voltammetric (CV) measurements were conducted between  $-0.6$  and  $0.8$  V vs Ag/AgCl at the potential scan rate of  $50$   $\text{mV s}^{-1}$  in  $0.1$   $\text{mol L}^{-1}$  phosphate buffer pH 7 in different gas environments (Ar-saturated, ambient air and O<sub>2</sub>-saturated).

*N<sub>2</sub> reduction reaction (NRR).* The reaction was carried out in  $60$   $\text{mL}$  of  $0.1$   $\text{mol L}^{-1}$  PBS pH 7 in which high purity N<sub>2</sub> gas or ambient air ( $30$   $\text{mL min}^{-1}$ ) was bubbled for  $45$  min for complete saturation of the medium, as well as throughout the entire electrolysis ( $2$  h). Before the gas injection, NH<sub>3</sub>/NO<sub>x</sub> impurities were removed from the gas feed using alkaline (NaOH  $5$   $\text{mmol L}^{-1}$ ) followed by acid (H<sub>2</sub>SO<sub>4</sub>  $5$   $\text{mmol L}^{-1}$ ) traps. The cell was based on the voltammetry cell, but with an insert with glass frit to separate the counter electrode compartment. Isotopic labelling experiments with <sup>15</sup>N<sub>2</sub> were conducted to validate nitrogen sources in the production of NH<sub>3</sub>. The experiment was carried out in  $0.1$   $\text{mol L}^{-1}$  PBS pH 7 with continuous purging of <sup>15</sup>N<sub>2</sub> ( $\geq 98$  atom % <sup>15</sup>N, Cambridge Isotope Laboratories, Inc.), applying a potential of  $-0.85$  V vs. Ag/AgCl for  $2$  h. Subsequently, the current density was recorded with respect to the geometric surface area of the working electrode,  $A = 0.5$   $\text{cm}^2$  considering front and back.

*H<sub>2</sub>O<sub>2</sub> detection.* For H<sub>2</sub>O<sub>2</sub> production, chronoamperometric curves were recorded in O<sub>2</sub>-saturated  $0.1$   $\text{mol L}^{-1}$  PBS pH 7 ( $60$   $\text{mL}$ ) at  $-0.6$  V vs Ag/AgCl for  $2$  h. Hydrogen peroxide detection was performing following a previously reported method.<sup>[61]</sup> Briefly, H<sub>2</sub>O<sub>2</sub> reacts with p-nitrophenyl boronic acid stoichiometrically in alkaline conditions (carbonate buffer pH 9) to give the product p-nitrophenol. The amount of p-nitrophenol, which equals the concentration of H<sub>2</sub>O<sub>2</sub>, is then detected and analysed using a LC-MS system. Thus, with a calibration curve (Figure S1) the concentration of H<sub>2</sub>O<sub>2</sub> is obtained.

*NH<sub>3</sub> detection.* The yield amount of NH<sub>3</sub> ( $[\text{NH}_3]_{\text{N}_2}$ ) in the solution was measured by LC-MS system. Before LC-MS analysis, the solution containing NH<sub>3</sub> was stained through the

indophenol method. Briefly, two reagent solutions were prepared: S1 was prepared by dissolving 100 mmol L<sup>-1</sup> phenol and 50 mg L<sup>-1</sup> sodium nitroprusside dihydrate in ultrapure water. S2 is composed of 0.38 mol L<sup>-1</sup> dibasic sodium phosphate, 125 mmol L<sup>-1</sup> sodium hydroxide, and 1% (vol) sodium hypochlorite (10-15 % active chlorine). Upon addition of the two reaction solutions (1000 μL each), the samples (200 μL) are mixed in and incubated at 37 °C for 40 min. All solutions and reactions should be stored at 4 °C until use for LC-MS analysis. A calibration curve for NH<sub>3</sub> was constructed (Figure S2), using the procedure described above in triplicate, on standard NH<sub>4</sub>Cl solutions prepared in 0.1 mol L<sup>-1</sup> PBS pH 7 media with NH<sub>4</sub><sup>+</sup> concentrations ranging from 0.00 to 100 μM.

To eliminate the possible exterior sources of contaminations the corresponding Ar-saturated ([NH<sub>3</sub>]<sub>Ar</sub>) condition and the open-circuit N<sub>2</sub>-saturated condition ([NH<sub>3</sub>]<sub>open</sub>) for the NRR experiment were used as the baseline for NH<sub>3</sub> production. Thus, the corrected [NH<sub>3</sub>] produced during the N<sub>2</sub> reduction was calculated using the following equation (Equation 1):

$$[NH_3] = [NH_3]_{N_2} - [NH_3]_{Ar} - [NH_3]_{open} \quad (S1)$$

The NH<sub>3</sub> yield rate was determined by (Equation 2):

$$NH_3 \text{ yield rate } (\mu\text{g h}^{-1} \text{ mg}_{cat}^{-1}) = ([NH_3] \times V)/(t \times m) \quad (S2)$$

Here [NH<sub>3</sub>] is the corrected concentration of NH<sub>3</sub> production (μg L<sup>-1</sup>); V is the volume of the electrolyte (L); m is the mass loading of the catalyst on CP (mg), and t is the electrolysis reaction time (h).

The Faradaic efficiency (FE) can be calculated using the following equation (Equation 3):

$$FE = (3 \times F \times [NH_3] \times V)/17 \times Q \quad (S3)$$

Here *F* refers to the Faraday constant (96485.3 C mol<sup>-1</sup>), *Q* is the quantity of electric charge via the applied potential during the entire experiment (C).<sup>[62]</sup>

*N<sub>2</sub>H<sub>4</sub> detection.* The Watt and Chrisp method was adopted to quantify the N<sub>2</sub>H<sub>4</sub> in the electrolyte after the reaction.<sup>[63]</sup> The coloring agent was prepared by mixing 6.0 g of *p*-C<sub>9</sub>H<sub>11</sub>NO with 30 mL of concentrated HCl and 300 mL of C<sub>2</sub>H<sub>5</sub>OH. Then, 5 mL of the electrolyte was taken from the acid trap and mixed with 5 mL of the coloring agent followed by stirring for 10 min and standing for 20 min. The absorbance of the solution was constructed using standard hydrazine hydrate solutions ranging from 5 to 35 μmol L<sup>-1</sup> M. As demonstrated in Figure S4, a good linear relationship between the absorbance value and the N<sub>2</sub>H<sub>4</sub> concentration was obtained in three independent calibrations.

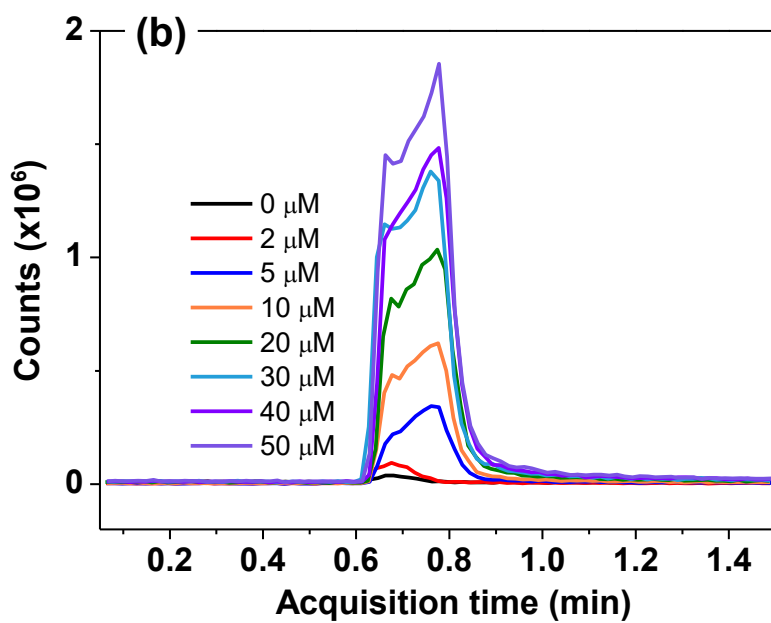
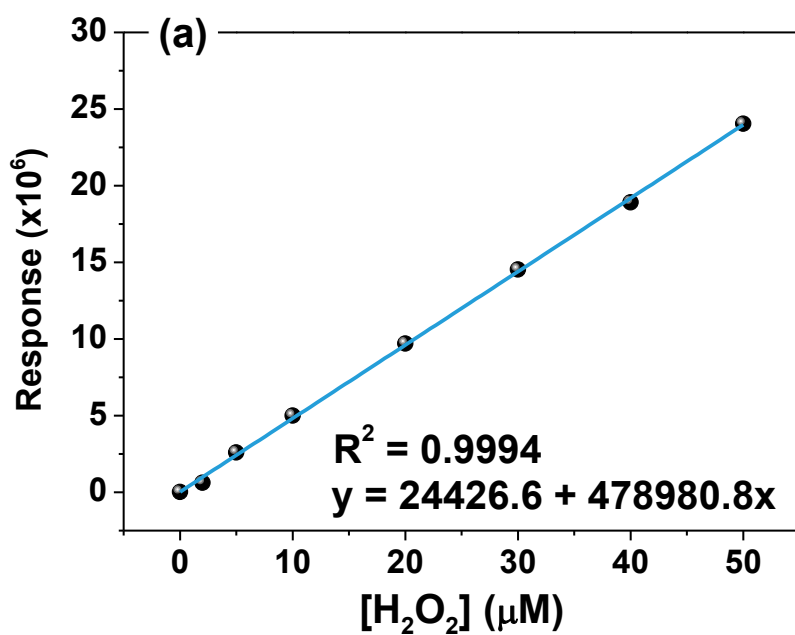


**Figure S1.** Calibration curve for estimating  $\text{H}_2\text{O}_2$  concentration, (b) corresponding counts versus acquisition time for LC-MS of resultant solutions.

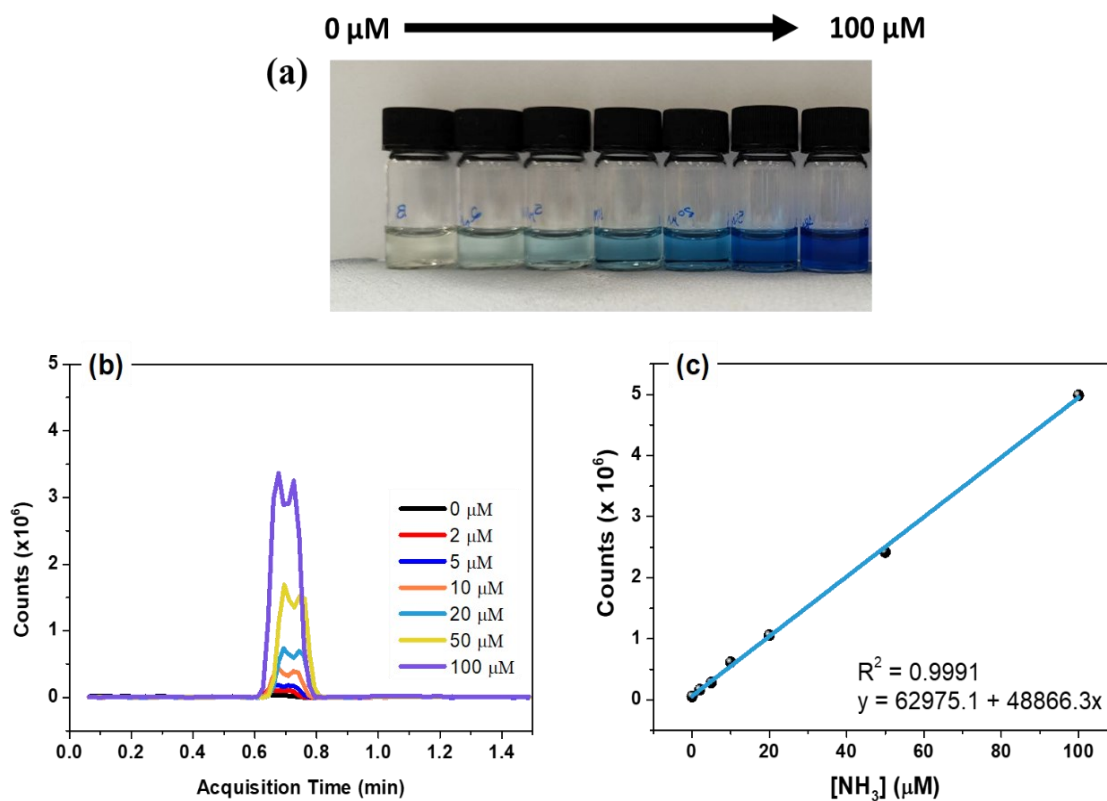


**Figure S2.** (a) Photograph of different concentrations of  $\text{NH}_3$  converted to the indophenol indicator, (b) corresponding counts versus acquisition time for LC-MS of resultant solutions and (c) calibration of the indophenol blue method for estimating  $\text{NH}_3$  concentration, using  $\text{NH}_4\text{Cl}$  solutions of known concentration as standards calibration.

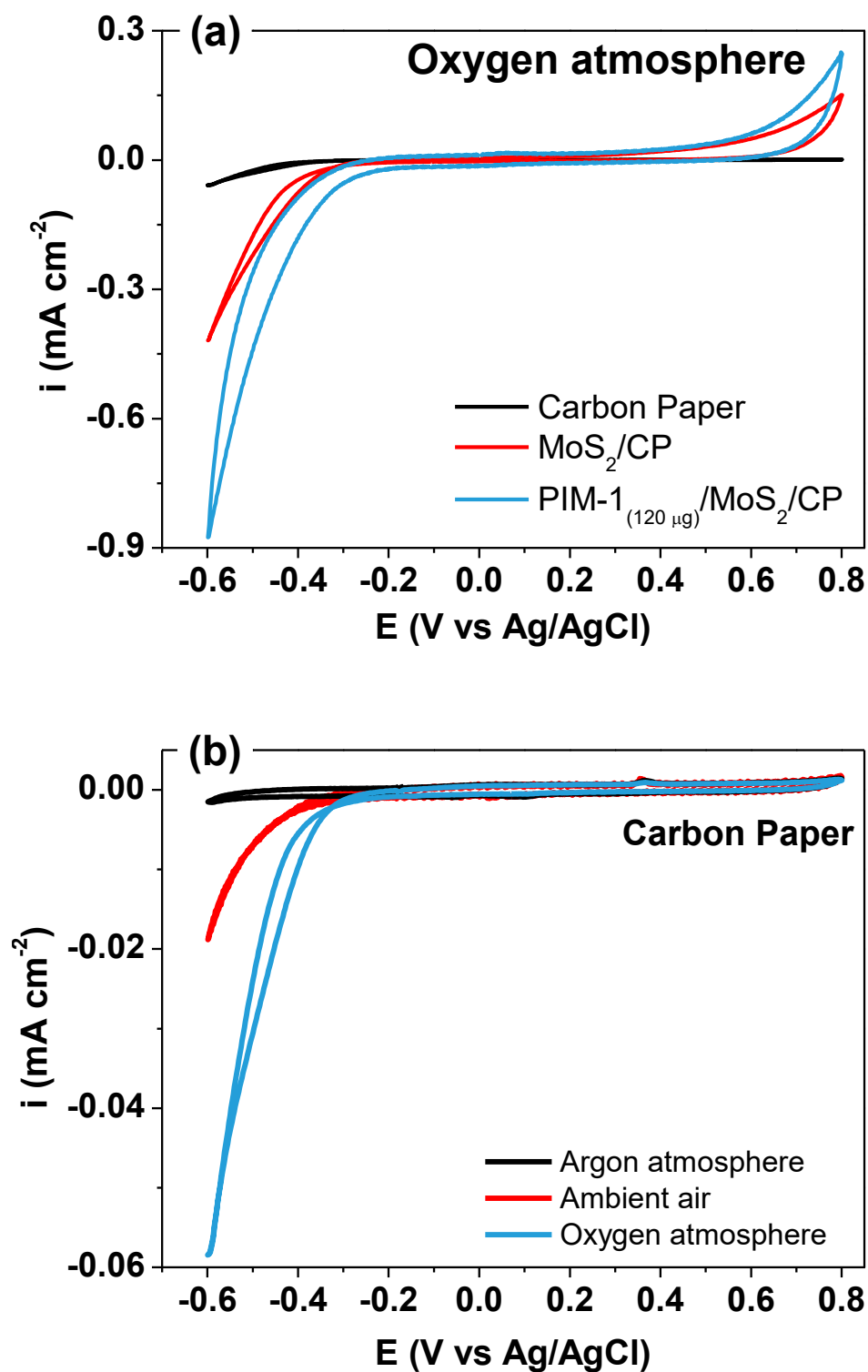


**Figure S3.** (a) Cyclic voltammograms (scan rate 50 mV s<sup>-1</sup>) for carbon paper, MoS<sub>2</sub>/CP and PIM-1<sub>(120 μg)</sub>/MoS<sub>2</sub> (inset) in O<sub>2</sub>-saturated 0.1 mol L<sup>-1</sup> phosphate buffer pH 7. (b) Cyclic voltammograms (scan rate 50 mV s<sup>-1</sup>) for carbon paper in 0.1 mol L<sup>-1</sup> phosphate buffer pH 7 at different gas environments.

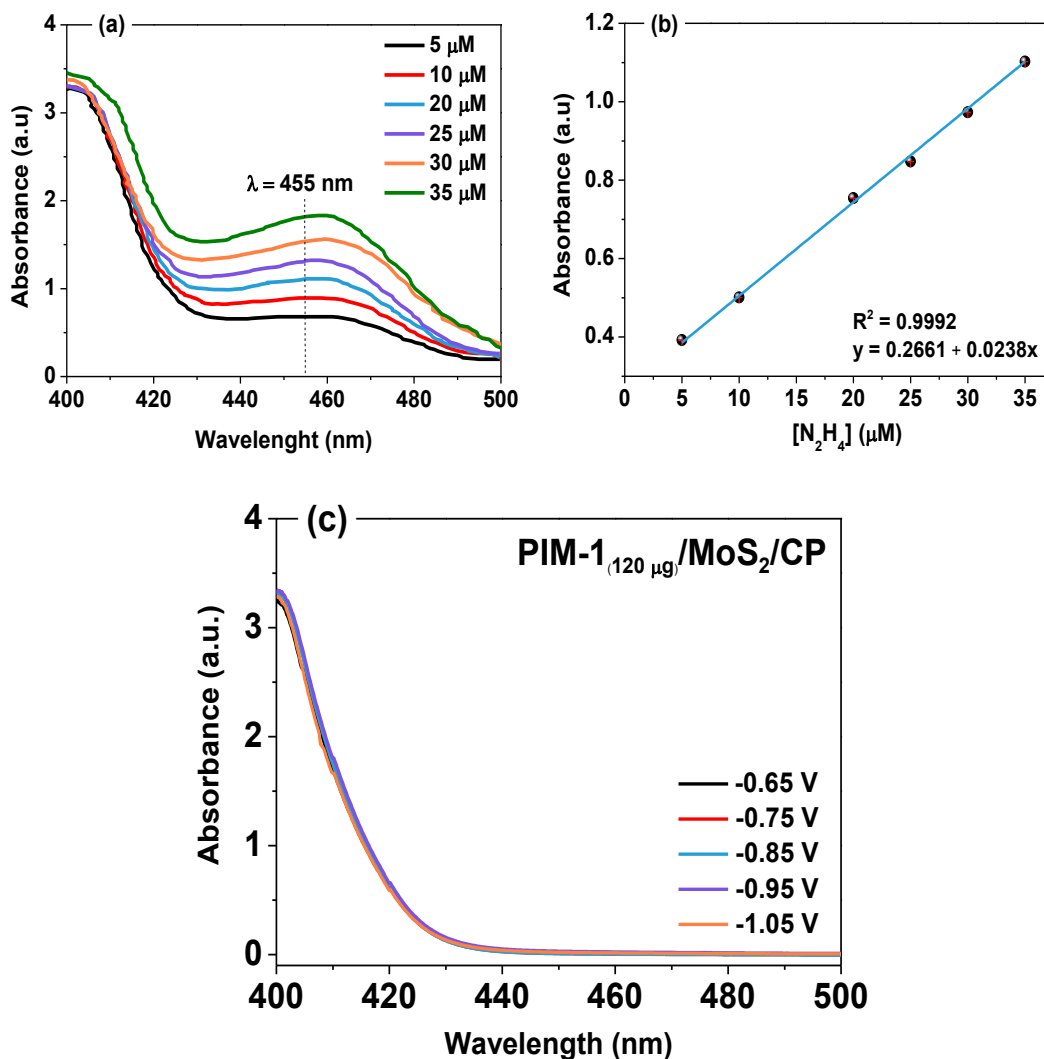


**Figure S4.** Calibration of the Watt and Chrisp method for estimating  $N_2H_4$  concentration, using  $N_2H_4$  solutions of known concentration as standards. (a) UV-Vis curves of various  $N_2H_4$  concentration after incubated for 30 min at room temperature. The absorbance at 455 nm was measured by UV-Vis spectrophotometer (b) calibration curve used for estimation of  $N_2H_4$  concentration. (c) UV-vis absorption spectra of the electrolyte stained with Watt and Chrisp indicator after NRR electrolysis using PIM-1<sub>(120  $\mu g$ )</sub>/MoS<sub>2</sub>/CP at -0.85 V vs. Ag/AgCl.

**Table S1.** Comparison of optimum NH<sub>3</sub> yield rates and faradaic efficiency (FE) for several catalysts for NRR at ambient conditions.

Catalyst	Electrolyte	Optimum Potential (V vs. RHE)	NH <sub>3</sub> yield rate (μg h <sup>-1</sup> mg <sup>-1</sup> )	FE (%)	Ref.
<b>PIM-1<sub>(120 μg)</sub>/MoS<sub>2</sub>/CP</b>	<b>0.1 M PBS</b>	<b>-0.24*</b>	<b>61.2</b>	<b>45.4</b>	<b>This work</b>
MoS <sub>2</sub> @Fe <sub>x</sub> O <sub>y</sub>	0.1 M Na <sub>2</sub> SO <sub>4</sub>	-0.2	62.6	54.9	[22]
FeMo <sub>3</sub> S <sub>4</sub> nanorods	0.5 M LiClO <sub>4</sub>	-0.3	65.3	19.2	[64]
Mo <sub>2</sub> C/C	0.5 M Li <sub>2</sub> SO <sub>4</sub>	-0.3	11.3	7.8	[65]
Mo <sub>2</sub> N nanorods	0.1 M HCl	-0.3	78.4	4.5	[66]
MoO <sub>2</sub> /graphene	0.1 M Na <sub>2</sub> SO <sub>4</sub>	-0.35	37.4	6.6	[67]
FeMoO <sub>4</sub> nanorods	0.5 M LiClO <sub>4</sub>	-0.5	45.8	13.2 (-0.3 V)	[68]
Mo <sub>3</sub> Fe <sub>3</sub> C	1 M KOH	-0.05	1.23	27	[69]
FeMoN <sub>6</sub>	0.25 M LiClO <sub>4</sub>	-0.3	14.95	41.7 (-0.2 V)	[70]
Defect rich MoS <sub>2</sub>	0.1 M Na <sub>2</sub> SO <sub>4</sub>	-0.4	29.28	8.34	[71]
MoS <sub>2</sub> -800	0.1 M HCl	-0.35	23.38	17.9	[72]
Metastable 1T'' MoS <sub>2</sub>	0.1 M Na <sub>2</sub> SO <sub>4</sub>	-0.3	9.24	13.4	[73]
S-rich MoS <sub>2</sub> nanosheet	0.1 M Li <sub>2</sub> SO <sub>4</sub>	-0.4	43.2	9.8	[74]
Fe <sub>2</sub> O <sub>3</sub> /Cu	0.1 M KOH	-0.1	15.60	24.40	[75]
NiWO <sub>4</sub>	0.1 M HCl	-0.3	40.05	19.32	[76]
Fe-Ni <sub>2</sub> P	0.1 M HCl	-0.3	88.51	7.95	[77]
Ag <sub>3</sub> Cu	0.1 M Na <sub>2</sub> SO <sub>4</sub>	-0.5	24.59	13.28	[78]

\* The potential was converted to the scale of the reversible hydrogen electrode (RHE) with the following equation:  $E$  (vs RHE) =  $E_{\text{appl}}$  (vs. Ag/AgCl/Cl<sub>(4M KCl)</sub>) + pH × 0.059 V + 0.197 V.

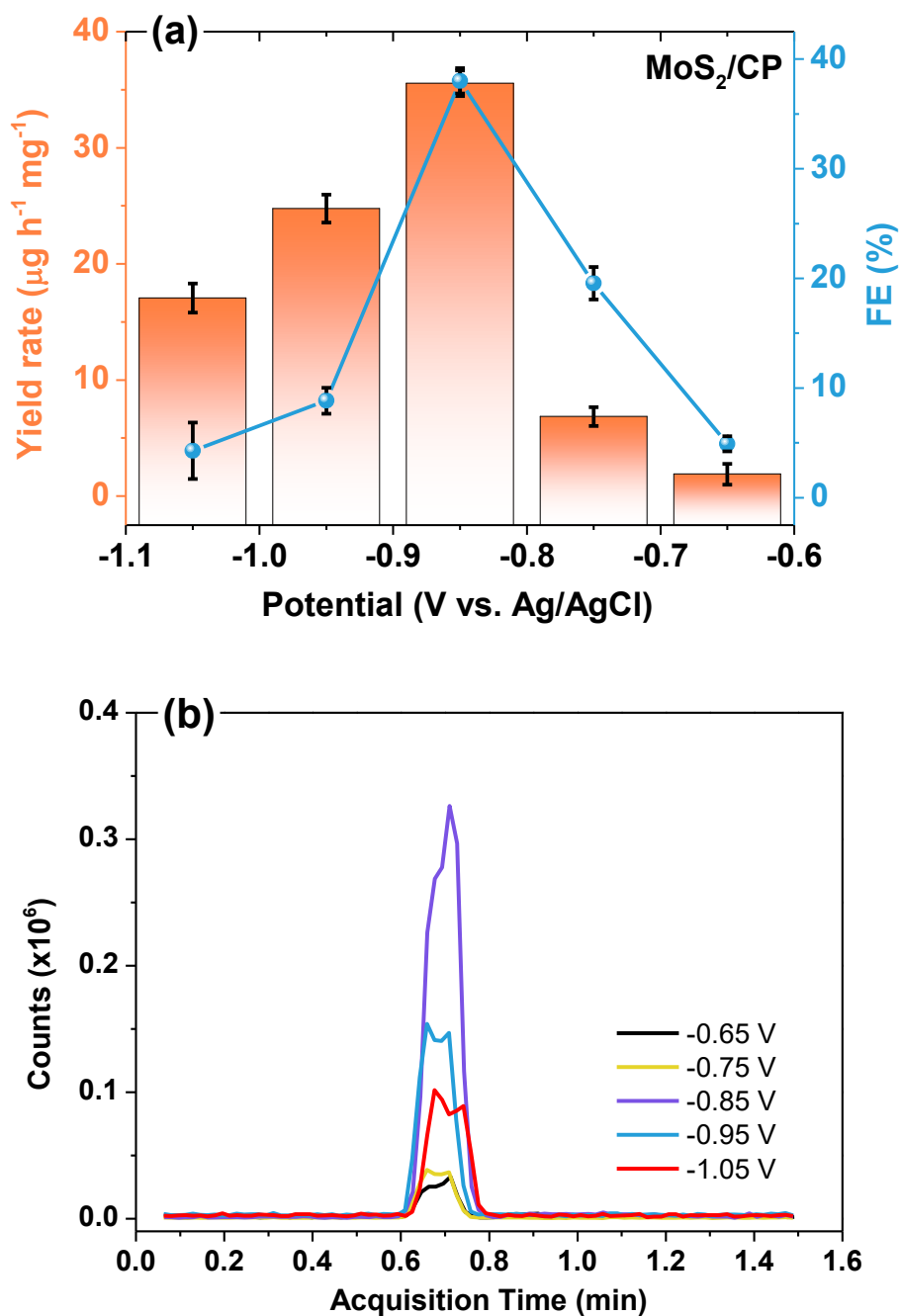


**Figure S5.** (a) NH<sub>3</sub> yield rate and FE values and (b) corresponding counts *versus* acquisition time for LC-MS of resultant electrolytes with indophenol indicator produced at different potentials for MoS<sub>2</sub>/CP catalyst.

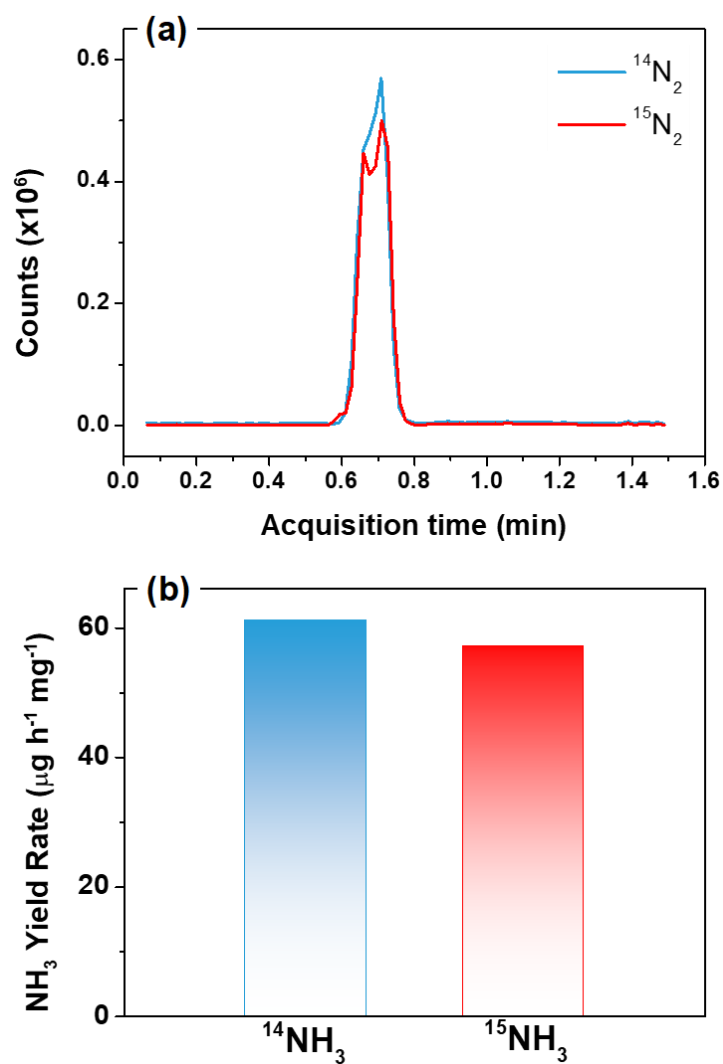


**Figure S6.** (a) Corresponding counts versus acquisition time for LC-MS peak integration data for indophenol indicator from ammonia and (b) NH<sub>3</sub> Yield rate comparison using <sup>14</sup>N<sub>2</sub> and <sup>15</sup>N<sub>2</sub> as the feeding gas for PIM-1(120 μg)/MoS<sub>2</sub>/CP at -0.85 V vs. Ag/AgCl.

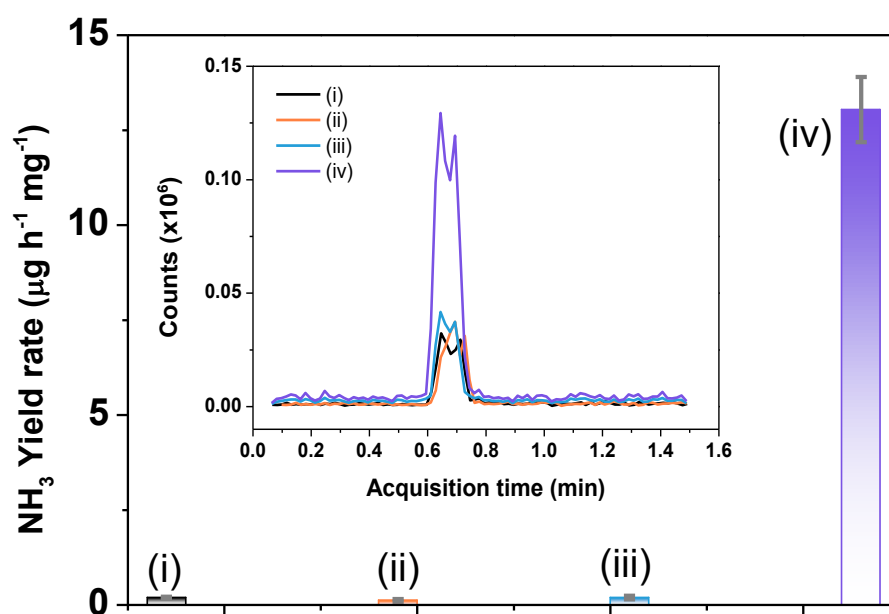


**Figure S7.** Comparison of  $\text{NH}_3$  yield rate and LC chromatogram peak integration for indophenol and MS mass signal (insert) for 2h electrolysis: (i) PBS 0.1 M under ambient air, (ii) using bare carbon paper electrodes in ambient air, (iii) without current flow under ambient air, and (iv) applying  $-0.85$  V vs. Ag/AgCl in PIM-1( $120 \mu\text{g}$ )/ $\text{MoS}_2$ /CP. In cases (i to iii), the ammonia detection remains negligible in comparison with reaction in PIM-1( $120 \mu\text{g}$ )/ $\text{MoS}_2$ /CP (iv).

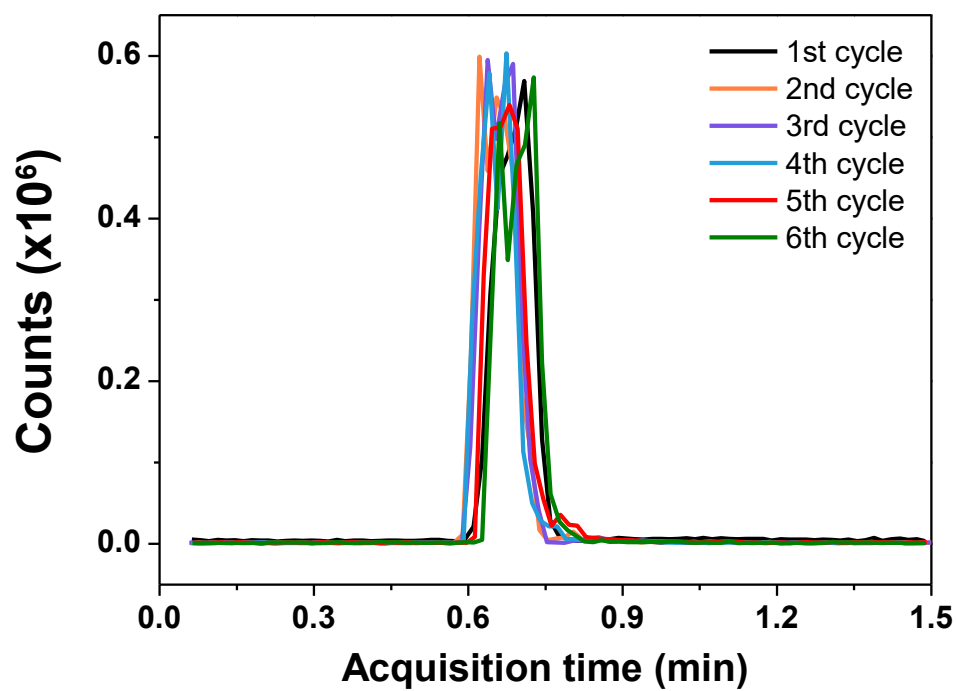


**Figure S8.** Counts *versus* acquisition time measurements after six chronoamperometric runs for PIM-1(120  $\mu$ g)/MoS<sub>2</sub>/CP at -0.85 V vs. Ag/AgCl.

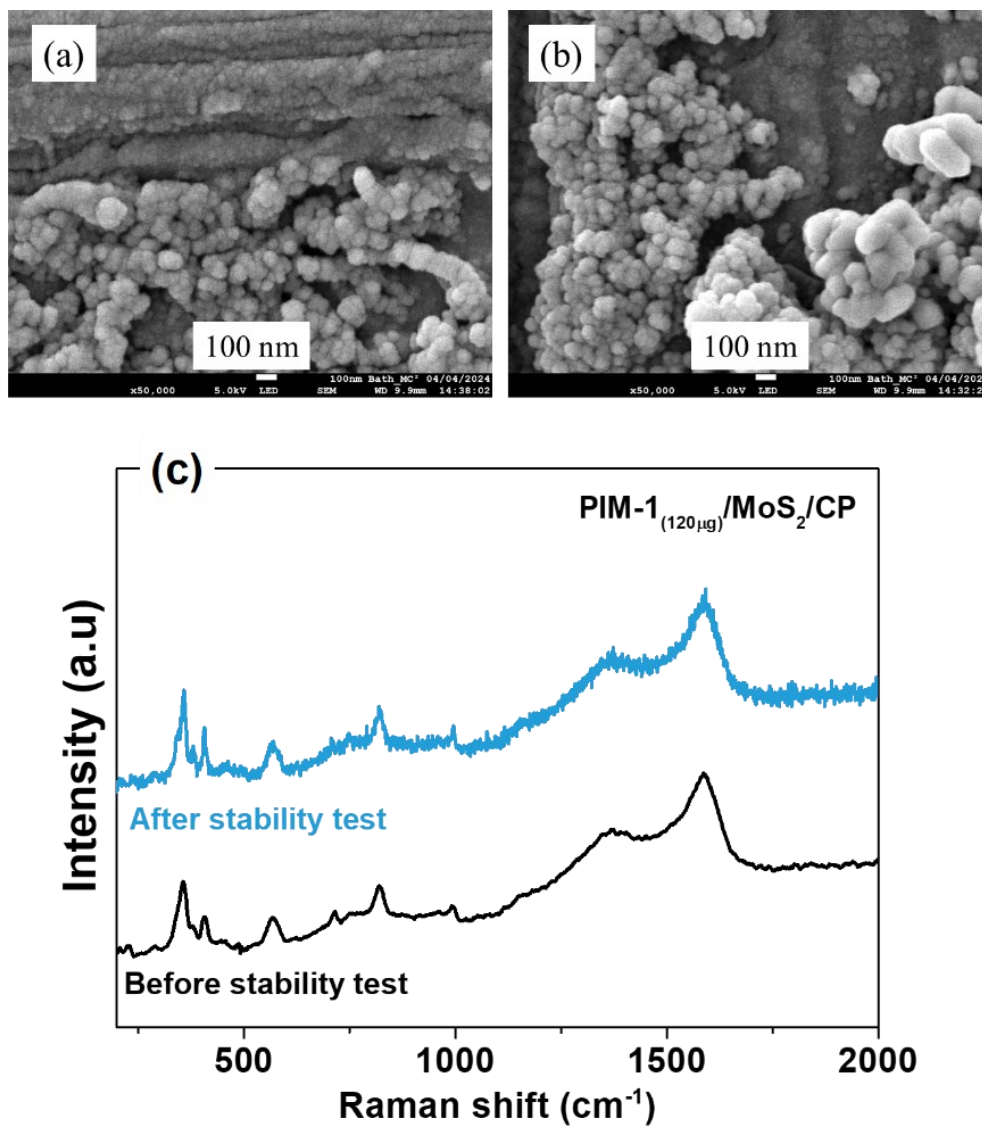


**Figure S9.** SEM images (a) before and (b) after stability test by 2h electrolysis and (c) Raman spectra (532 nm) before and after stability test for PIM-1<sub>(120 μg)</sub>/MoS<sub>2</sub>/CP.

## References

- 56 P.M. Budd, E.S. Elabas, B.S. Ghanem, S. Makhseed, N.B. McKeown, K.J. Msayib, C.E. Tattershall and D. Wang, *Adv. Mater.*, 2004, **16**, 456.
- 57 P.M. Budd, B.S. Ghanem, S. Makhseed, N.B. McKeown, K.J. Msayib and C.E. Tattershall, *Chem. Commun.*, 2004, 230.
- 58 M. Medina, P.G. Corradini and L.H. Mascaro, *J. Braz. Chem. Soc.*, 2019, **30**, 2210.
- 59 M. Vizza, W. Giurlani, L. Cerri, N. Calisi, A. A. Leonardi, M. J. L. Faro, A. Irrera, E. Berretti, J. V. Perales-Rondón, A. Colina, E. B. Saiz and M. Innocenti, *Molecules*, 2022, **27**, 5416.
- 60 C.V.S. Almeida and L.H. Mascaro, *Electrochim. Acta*, 2024, **476**, 143680.
- 61 L. Wang, M. Carta, R. Malpass-Evans, N.B. McKeown, P.J. Fletcher, P. Estrela, A. Roldan and F. Marken, *J. Catal.*, 2022, **416**, 253.
- 62 S.Z. Andersen, V. Colic, S. Yang, J.A. Schwalbe, A.C. Nielander, J.M. McEnaney, K. Enemark-Rasmussen, J.G. Baker, A.R. Singh, B.A. Rohr, M.J. Statt, S.J. Blair, S. Mezzavilla, J. Kibsgaard, P.C.K. Vesborg, M. Cargnello, S.F. Bent, T.F. Jaramillo, I.E.L. Stephens, J.K. Norskov and I. Chorkendorff, *Nature*, 2019, **570**, 504.
- 63 T. Wu, P. Li, H. Wang, R. Zhao, Q. Zhou, W. Kong, M. Liu, Y. Zhang, X. Sun and Feng Gong, *Chem. Commun.*, 2019, **55**, 2684.
- 64 J. Wang, H. Nan, Y. Tian and K. Chu, *ACS Sustain. Chem. Eng.*, 2020, **8**, 12733.
- 65 H. Cheng, L. X. Ding, G. F. Chen, L. Zhang, J. Xue and H. Wang, *Adv. Mater.*, 2018, **30**, 1803694.
- 66 X. Ren, G. Cui, L. Chen, F. Xie, Q. Wei, Z. Tian and X. Sun, *Chem. Commun.*, 2018, **54**, 8474.
- 67 J. Wang, Y. P. Liu, H. Zhang, D. J. Huang and K. Chu, *Catal. Sci. Technol.*, 2019, **9**, 4248.
- 68 K. Chu, Q. Q. Li, Y. H. Cheng and Y. P. Liu, *ACS Appl. Mater. Inter.*, 2020, **12**, 11789.
- 69 H. Cheng, P. X. Cui, F. R. Wang, L. X. Ding and H. H. Wang, *Angew. Chem. Int. Ed.* 2019, **58**, 15541.
- 70 Y. Li, Q. Zhang, C. Li, H.-N. Fan, W.-B. Luo, H.-K. Liu and S.-X. Dou, *J. Mater. Chem. A*, 2019, **7**, 22242.
- 71 X. Li, T. Li, Y. Ma, Q. Wei, W. Qiu, H. Guo, X. Shi, P. Zhang, A.M. Asiri, L. Chen, B. Tang and X. Sun, *Adv. Energy Mater.*, 2018, **8**, 1801357.
- 72 M. You, S. Yi, X. Hou, Z. Wang, H. Ji, L. Zhang, Y. Wang, Z. Zhang and D. Chen, *J. Colloid Interface Sci.*, 2021, **599**, 849e856.
- 73 G. Lin, Q. Ju, X. Guo, W. Zhao, S. Adimi, J. Ye, Q. Bi, J. Wang, M. Yang and F. Huang, *Adv. Mater.*, 2021, **33**, 2007509.
- 74 Y. Liu, M. Han, Q. Xiong, S. Zhang, C. Zhao, W. Gong, G. Wang, H. Zhang and H. Zhao, *Adv. Mater.*, 2019, **9**, 1803935.
- 75 C. Huang, L. Shang, P. Han, Z. Gu, A. M. Al-Enizi, T. M. Almutairi, N. Cao and G. Zheng, *J. Colloid Interface Sci.*, 2019, **552**, 312.
- 76 J. Wang, H. Jang, G. Li, M. G. Kim, Z. Wu, X. Liu and J. Cho, *Nanoscale*, 2020, **12**, 1478.
- 77 C. Guo, X. Liu, L. Gao, X. Kuang, X. Ren, X. Ma, M. Zhao, H. Yang, X. Sun and Q. Wei, *Appl. Catal. B: Environ.*, 2020, **263**, 118296.
- 78 H. Yu, Z. Wang, D. Yang, X. Qian, Y. Xu, X. Li, H. Wang and L. Wang, *J. Mater. Chem. A*, 2019, **7**, 12526.